nature astronomy

LETTERS

DOI: 10.1038/s41550-017-0216-z

Dynamical dark energy in light of the latest observations

Gong-Bo Zhao[1,2*], Marco Raveri[3,4], Levon Pogosian[2,5], Yuting Wang[1,2], Robert G. Crittenden[2], Will J. Handley[6,7], Will J. Percival[2], Florian Beutler[2], Jonathan Brinkmann[8], Chia-Hsun Chuang[9,10], Antonio J. Cuesta[11,12], Daniel J. Eisenstein[13], Francisco-Shu Kitaura[14,15], Kazuya Koyama[2], Benjamin L'Huillier[16], Robert C. Nichol[2], Matthew M. Pieri[17], Sergio Rodriguez-Torres[9,18,19], Ashley J. Ross[2,20], Graziano Rossi[21], Ariel G. Sánchez[22], Arman Shafieloo[16,23], Jeremy L. Tinker[24], Rita Tojeiro[25], Jose A. Vazquez[26] and Hanyu Zhang[1]

A flat Friedmann–Robertson–Walker universe dominated by a cosmological constant (Λ) and cold dark matter (CDM) has been the working model preferred by cosmologists since the discovery of cosmic acceleration[1,2]. However, tensions of various degrees of significance are known to be present among existing datasets within the ΛCDM framework[3–11]. In particular, the Lyman-α forest measurement of the baryon acoustic oscillations (BAO) by the Baryon Oscillation Spectroscopic Survey[3] prefers a smaller value of the matter density fraction Ω_M than that preferred by cosmic microwave background (CMB). Also, the recently measured value of the Hubble constant, $H_0 = 73.24 \pm 1.74\,\mathrm{km\,s^{-1}\,Mpc^{-1}}$ (ref. [12]), is 3.4σ higher than the $66.93 \pm 0.62\,\mathrm{km\,s^{-1}\,Mpc^{-1}}$ inferred from the Planck CMB data[7]. In this work, we investigate whether these tensions can be interpreted as evidence for a non-constant dynamical dark energy. Using the Kullback–Leibler divergence[13] to quantify the tension between datasets, we find that the tensions are relieved by an evolving dark energy, with the dynamical dark energy model preferred at a 3.5σ significance level based on the improvement in the fit alone. While, at present, the Bayesian evidence for the dynamical dark energy is insufficient to favour it over ΛCDM, we show that, if the current best-fit dark energy happened to be the true model, it would be decisively detected by the upcoming Dark Energy Spectroscopic Instrument survey[14].

The observational datasets considered in this work include the latest cosmic microwave background (CMB) temperature and polarization anisotropy spectra, the supernovae (SNe) luminosity distance data, the baryon acoustic oscillations (BAO) angular diameter distance data from the clustering of galaxies (gBAO) and from the Lyman-α forest (LyαFB), the estimate of the current value of the Hubble constant (H_0), the measurements of the Hubble parameter $H(z)$ at redshifts z using the relative age of old and passively evolving galaxies (OHD), the three-dimensional galaxy power spectra and the two-dimensional weak-lensing shear angular power spectra. Further details about the datasets and associated systematic effects can be found in the Methods.

The Kullback–Leibler (KL) divergence, also known as relative entropy, quantifies the proximity of two probability density functions (PDFs). Rather than focusing on particular model parameters, it is designed to compare the overall concordance of datasets within a given model. We use the difference between the actual and the expected KL divergence, called 'Surprise'[15], as a measure of tension between datasets. Rather than comparing the PDFs for the Λ cold dark matter model (ΛCDM, where Λ is the cosmological constant) parameters for every pair of datasets, we take the combined dataset, ALL16 (see Supplementary Table 1), and find the derived PDFs for the angular diameter distance $D_A(z)$ and $H(z)$ at redshifts corresponding to the available data. We then compute the KL divergence between the derived PDFs and the directly observed $D_A(z)$

[1]National Astronomical Observatories, Chinese Academy of Sciences, Beijing 100012, China. [2]Institute of Cosmology and Gravitation, University of Portsmouth, Portsmouth PO1 3FX, UK. [3]Kavli Institute for Cosmological Physics, Enrico Fermi Institute, The University of Chicago, Chicago, IL 60637, USA. [4]Institute Lorentz, Leiden University, PO Box 9506, Leiden 2300 RA, Netherlands. [5]Department of Physics, Simon Fraser University, Burnaby, BC V5A 1S6, Canada. [6]Astrophysics Group, Cavendish Laboratory, J. J. Thomson Avenue, Cambridge CB3 0HE, UK. [7]Kavli Institute for Cosmology, Madingley Road, Cambridge CB3 0HA, UK. [8]Apache Point Observatory, PO Box 59, Sunspot, NM 88349, USA. [9]Instituto de Física Teórica, (UAM/CSIC), Universidad Autónoma de Madrid, Cantoblanco, Madrid E-28049, Spain. [10]Leibniz-Institut für Astrophysik Potsdam (AIP), An der Sternwarte 16, 14482 Potsdam, Germany. [11]Institut de Ciències del Cosmos (ICCUB), Universitat de Barcelona (IEEC- UB), Martí i Franquès 1, Barcelona E-08028, Spain. [12]Departamento de Física, Universidad de Córdoba, Campus de Rabanales, Edificio Albert Einstein, Córdoba E-14071, Spain. [13]Harvard-Smithsonian Center for Astrophysics, 60 Garden Street, Cambridge, MA 02138, USA. [14]Instituto de Astrofísica de Canarias, 38205 San Crist obal de La Laguna, Santa Cruz de Tenerife, Spain. [15]Departamento de Astrofísica, Universidad de La Laguna (ULL), La Laguna, Tenerife E-38206, Spain. [16]Korea Astronomy and Space Science Institute, 776 Daedeokdae-ro, Yuseong-gu, Daejeon 34055, Korea. [17]Aix Marseille Université, CNRS, Laboratoire d'Astrophysique de Marseille, UMR 7326, Marseille 13388, France. [18]Campus of International Excellence UAM+CSIC, Cantoblanco, Madrid E-28049, Spain. [19]Departamento de Física Teórica, Universidad Autónoma de Madrid, Cantoblanco, Madrid E-28049, Spain. [20]Center for Cosmology and AstroParticle Physics, The Ohio State University, Columbus, OH 43210, USA. [21]Department of Astronomy and Space Science, Sejong University, Seoul 143-747, Korea. [22]Max-Planck-Institut für extraterrestrische Physik, Postfach 1312, Giessenbachstraße, 85741 Garching, Germany. [23]University of Science and Technology, 217 Gajeong-ro, Yuseong-gu, Daejeon 34113, Korea. [24]Center for Cosmology and Particle Physics, Department of Physics, New York University, 4 Washington Place, New York, NY 10003, USA. [25]School of Physics and Astronomy, University of St Andrews, North Haugh, St Andrews KY16 9SS, UK. [26]Brookhaven National Laboratory, Building 510, Upton, NY 11973, USA. *e-mail: gbzhao@nao.cas.cn

and $H(z)$ from H_0, SNe, OHD, gBAO and LyαFB, and evaluate the corresponding Surprise and the standard deviation (see Methods for details). Results are shown as cyan bars in Fig. 1a. They indicate that the H_0, LyαFB and SNe measurements are in tension with the combined dataset. Introducing tension T as the number of standard deviations by which Surprise is greater than zero, we find values of $T=4.4$, 3.5 and 1.7 for the H_0, LyαFB and SNe measurements, respectively (shown in Fig. 1b), with the first two values signalling significant tension.

Next, we check whether the tension within the ΛCDM model can be interpreted as evidence for a dynamical dark energy. The dynamics of dark energy can be probed in terms of its equation of state w, which is equal to -1 for Λ, but is different in dynamical dark energy models, where it will generally be a function of redshift z. Commonly considered alternatives to Λ are a model with a constant w (wCDM) and one in which w is a linear function of the scale factor (w_0w_aCDM)[16]. We allow for a general evolution of the dark energy equation of state and use the correlated prior probability distribution method[17] (hereafter, the prior probability distribution is simply called the 'prior') to perform a Bayesian non-parametric reconstruction of $w(z)$ using the Markov chain Monte Carlo method with other cosmological parameters marginalized over (see Methods for details). Figure 2 presents the reconstructed $w(z)$, along with the 68% confidence-level uncertainty, shown with a light blue band, derived from the combined dataset ALL16. Table 1 shows the change in χ^2 relative to ΛCDM for each individual dataset for the best-fit $w(z)$CDM model derived from ALL16. Overall, the χ^2 is improved by -12.3, which can be interpreted as the reconstructed dynamical dark energy model being preferred at 3.5σ. The reconstructed dark energy equation of state evolves with time and crosses the -1 boundary, which is prohibited in single-field minimally coupled quintessence models[18], but can be realized in models with multiple scalar fields, such as Quintom[19], or if the dark energy field mediates a new force between matter particles[20]. In the latter case, which is commonly classified as modified gravity, it is generic for the effective dark energy equation of state to be close to -1 around $z=0$, but to evolve towards more negative values at intermediate redshifts, before eventually approaching 0 during matter domination. Such dynamics would be consistent with our reconstruction and could be tested in the future when BAO measurements at higher redshifts become available. In addition to the reconstruction from the combined ALL16 dataset presented in Fig. 2, we present reconstructions derived from ten different data combinations in Supplementary Fig. 1.

The results for tension between datasets, re-evaluated for the ALL16 best-fit $w(z)$CDM model, are shown as dark blue bars in Fig. 1. We find $T=0.7$, 1.1 and 0.7 for H_0, LyαFB and SNe, respectively, indicating that tensions that existed in the ΛCDM model are significantly released within $w(z)$CDM. A plot of the relevant data points along with the best-fit predictions from the ΛCDM and the $w(z)$CDM models are provided in Supplementary Fig. 2.

With a large number of additional w-bin parameters, one may be concerned that the improvement in the fit is achieved by $w(z)$CDM at the cost of a huge increase in the parameter space. However, correlations between the w-bins induced by the prior constrain most of that freedom. One way to estimate the effective number of additional degrees of freedom is to perform a principal-component analysis of the posterior covariance matrix of the w-bin parameters and compare it with that of the prior. Using this method, explained in detail in the Methods section, we find that our $w(z)$CDM model effectively has only four additional degrees of freedom compared with ΛCDM. We note that the demonstration that ALL16 is capable of constraining four principal components of $w(z)$ is one of the interesting results of this work.

It is interesting to compare $w(z)$ reconstructed from ALL16 with that obtained by Zhao et al.[21] using the same prior but a different dataset, which we call ALL12 (a comparison of the ALL16 and the ALL12 datasets is provided in Supplementary Table 2). ALL16 contains about 40% more SNe than ALL12, primarily provided by the Sloan Digital Sky Survey (SDSS)-II. Moreover, in ALL12, the BAO measurement derived from the Baryon Oscillation Spectroscopic Survey (BOSS) DR9 sample[22] was at a single effective redshift, whereas in ALL16 it is tomographic at nine redshifts from BOSS DR12 (ref. [23]), which contains four times more galaxies than DR9. In addition, ALL16 includes a high-redshift LyαFB measurement,

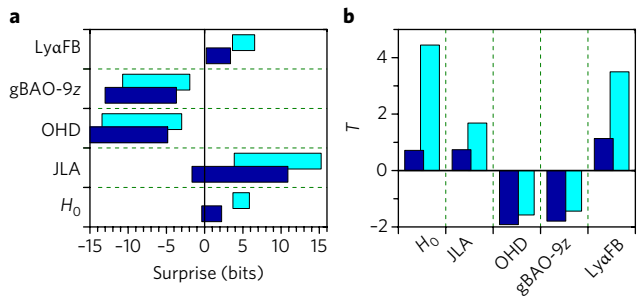

Fig. 1 | The tension among different datasets in ΛCDM and $w(z)$CDM universes. a, The Surprise between the PDFs for $D_A(z)$ and $H(z)$ derived from the best-fit model using the combined dataset of ALL16, and the directly observed $D_A(z)$ and $H(z)$ from H_0, JLA (the JLA sample of SNe), OHD, gBAO-9z (gBAO measurements at nine effective redshifts) and LyαFB, respectively (see Methods for detailed explanation and references for data used). The cyan horizontal bars indicate the 68% confidence-level range of Surprise in ΛCDM, while the dark blue bars correspond to that of $w(z)$CDM. **b**, The corresponding values of tension T, defined as Surprise divided by its standard deviation, shown using the same colour scheme as in **a**.

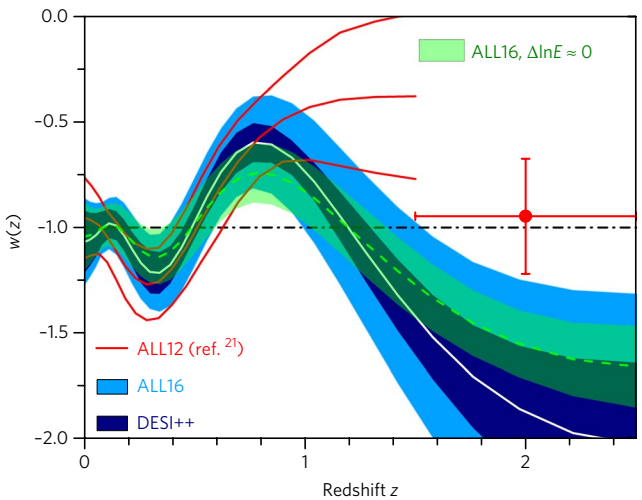

Fig. 2 | Reconstructed evolution history of the dark energy equation of state compared with the 2012 result and the forecasted uncertainty from future data. The mean (white solid) and the 68% confidence level (CL) uncertainty (light blue band) of the $w(z)$ reconstructed from ALL16 compared with the ALL12 $w(z)$ reconstructed by Zhao et al. (ref. [21]) (red lines show the mean and the 68% CL band). The red point with 68% CL error bars is the value of $w(z)$ at $z=2$ 'predicted' by the ALL12 reconstruction. The dark blue band around the ALL16 reconstruction is the forecasted 68% CL uncertainty from DESI++. The green dashed curve and the light green band show the mean and the 68% CL of $w(z)$, respectively, reconstructed from ALL16 using a different prior strength ($\sigma_D=0.4$), for which the Bayesian evidence is equal to that of ΛCDM. See the text for details.

Table 1 | The improved χ^2 with respect to that of the ΛCDM model

	P15	JLA	gBAO	$P(k)$	WL	H_0	LyαFB	OHD
$\chi^2_{w(z)\mathrm{CDM}}-\chi^2_{\Lambda\mathrm{CDM}}$	−0.7	−1.6	−2.8	+1.1	−0.1	−2.9	−3.7	−2.3
$\chi^2_{w\mathrm{CDM}}-\chi^2_{\Lambda\mathrm{CDM}}$	0.0	+0.5	+0.7	+0.4	+0.2	−2.9	−0.2	0.0
$\chi^2_{w_0w_a\mathrm{CDM}}-\chi^2_{\Lambda\mathrm{CDM}}$	−0.7	+0.4	+0.9	+0.5	+0.4	−2.7	−0.3	0.0

The changes in χ^2 of individual datasets between the ALL16 best-fit $w(z)$CDM, wCDM and w_0w_aCDM models and the ΛCDM model.

which was not available in 2012. This helps to constrain $w(z)$ at redshifts where the SNe constraints are weak. The new H_0 measurement in 2016 (ref. [12]) is consistent with that in 2009 (ref. [24]), with the error bar halved. Comparing measurements of the expansion rate and the cosmic distances in ALL12 and ALL16, we find that those in ALL16 offer information at a greater number of redshift values, and with a greater signal-to-noise ratio (see Supplementary Fig. 4 for a visual comparison). Quantitatively, the signal-to-noise ratio in measurements of $H(z)$, $D_A(z)$ and $d_L(z)$ in ALL16 is larger by 80%, 260% and 90%, respectively, than in those of the ALL12 dataset, where $d_L(z)$ is the luminosity distance. The Planck 2015 CMB data is also much more informative than the Wilkinson Microwave Anisotropy Probe seven-year release[25], thanks to a higher angular resolution of the temperature and polarization maps, and lower levels of statistical uncertainties.

Overall, ALL16 is more constraining due to a significant level of new and independent information in ALL16 compared with ALL12: the effective number of $w(z)$ degrees of freedom constrained by ALL12 was three, compared with four constrained by ALL16. Figure 2 compares the two results and shows that they are highly consistent. We quantify the agreement by evaluating the dot product of the $\hat{w}$ vectors from the two reconstructions (the vectors are normalized so that a dot product is unity if they are identical) and find that $\hat{w}_{\mathrm{ALL12}}\cdot\hat{w}_{\mathrm{ALL16}}=0.94\pm0.02$. We also evaluate the tension T between the two reconstruction results and find that $T=-1.1$. This indicates an excellent alignment of the two results. This agreement, and the raised significance of an evolving $w(z)$ from 2.5σ to 3.5σ confidence levels with more advanced observations, suggest the possibility of revealing the dynamics of dark energy at a much more statistically significant level in the near future, as we will present later.

To check whether the improvement in the fit warrants introducing additional effective degrees of freedom, we evaluate and compare the Bayesian evidence, $E\equiv\int \mathrm{d}\theta\mathcal{L}(\mathrm{D}|\theta)\mathrm{P}(\theta)$, for the ΛCDM and the $w(z)$CDM models. The Bayes factors, which are the differences in $\ln E$ between the two models, are shown in Table 2. The Bayes factors for both the ALL12 and the ALL16 dark energy models are negative, indicating that ΛCDM is favoured by this criterion. However, our forecast for a future dataset, DESI++, comprised of BAO measurements from the Dark Energy Spectroscopic Instrument (DESI)[14], around 4,000 SNe luminosity distances from future surveys[26] and the CMB (assuming Planck sensitivity), predicts a Bayes factor of 11.3 ± 0.3 if the ALL16 $w(z)$CDM reconstruction happened to be the true model, which would be decisive according to the Jeffreys scale.

Table 2 | The significance of $w\neq-1$ and Bayes factors

	ALL12	ALL16	DESI++
Signal-to-noise ratio	2.5σ	3.5σ	6.4σ
$\ln(E_{w(z)\mathrm{CDM}}/E_{\Lambda\mathrm{CDM}})$	-6.7 ± 0.3	-3.3 ± 0.3	11.3 ± 0.3

The statistical significance in terms of the standard deviation σ, that is, the signal-to-noise ratio defined as $\sqrt{\Delta\chi^2}$, of $w(z)$ deviating from −1 based on the improvement in the fit alone, and the Bayes factor $\Delta\ln E$ between the $w(z)$CDM models and the ΛCDM model, derived from the ALL12 and the ALL16 datasets respectively, along with the forecast for DESI++.

One may ask how much the evidence for dark energy depends on the particular choice of the prior parameters. In principle, the choice of the smoothing scale should be guided by theory. The value used by Zhao et al.[21] and in this work, $a_c=0.06$, where a_c describes the typical smoothing scale, is a timescale conservatively chosen to be sufficiently small so as not to bias reconstructions of $w(z)$ expected in quintessence dark energy models[17]. For the inference to be conclusive, the evidence for a dynamical dark energy should be strong over a wide range of the prior parameters. Therefore, we vary the strength of our prior by adjusting σ_D, which is a parameter added to the diagonal of the inverse of the prior covariance matrix, and examine how the significance of the dynamical dark energy detection, as well as the Bayesian evidence, change with the variation of σ_D. As shown in Fig. 3, and with additional details given in the Methods section, we find that neither ALL12 nor ALL16 provides evidence for a dynamical dark energy over the considered wide range of prior strengths. However, the Bayes factor for ALL16 is generally much

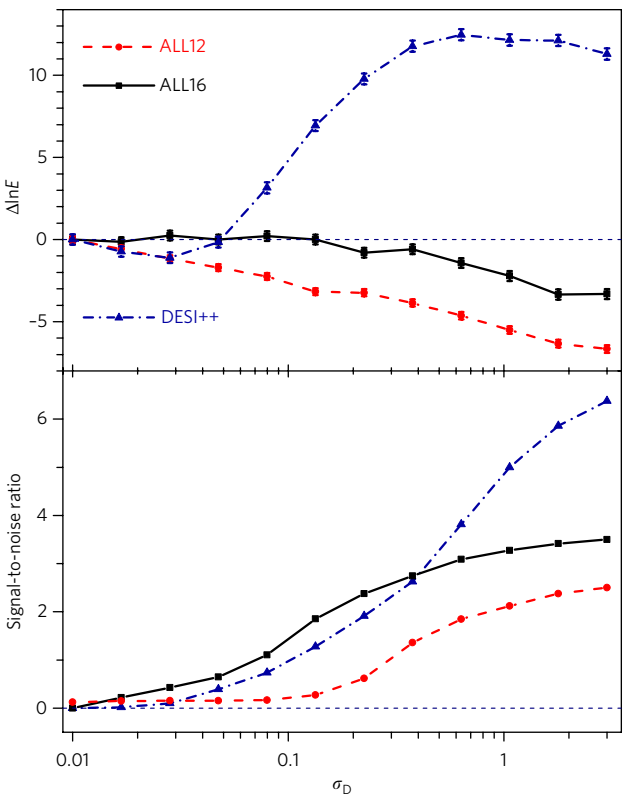

Fig. 3 | The Bayes factor and the significance level of $w\neq-1$ for various correlated priors for current and future data. The Bayes factor with 68% confidence-level error bars (upper panel) and the statistical significance (lower panel) of dynamical dark energy derived from the 2012 data (ALL12; red dashed)[21], current data (ALL16; black solid) and future data (DESI++; blue dot-dashed)[14]. Error bars show standard deviation.

Table 3 | Results for extended models

	M_1	M_2	M_3	M_4	M_5
Definition	$M_\nu = 0.06$ eV	$M_\nu, N_{\rm eff}$	$A_{\rm Lens}$	wCDM	w_0w_aCDM
Signal-to-noise ratio	3.6σ	3.4σ	3.4σ	3.5σ	3.4σ
$\Delta\ln E$	-2.8 ± 0.3	-3.9 ± 0.3	-3.6 ± 0.3	-0.9 ± 0.3	0.7 ± 0.3

The statistical significance, signal-to-noise ratio $=\sqrt{\Delta\chi^2}$, of the preference for $w(z)$CDM over ΛCDM with added parameters (M_1, M_2, M_3), and over a model with a constant w (that is, M_4) and one with a linearly varying $w(a)$ (that is, M_5). M_1 denotes a model with $M_\nu = 0.06$ eV, M_2 contains varying M_ν and $N_{\rm eff}$, and M_3 includes a varying $A_{\rm Lens}$. For M_1, M_2 and M_3, the new parameters are added to both $w(z)$ CDM and ΛCDM. The last row shows the Bayes factors, $\Delta\ln E$, between $w(z)$CDM and the five extended models.

less negative than that for ALL12 for all prior strengths. For example, the Bayes factor inferred from ALL12 increased from -6.7 ± 0.3 to -3.3 ± 0.3 for $\sigma_{\rm D}=3$, which is the prior used in this work. In fact, for ALL16, the Bayes factor remains close to zero for $\sigma_{\rm D}\lesssim0.4$. We plot the model with $\sigma_{\rm D}=0.4$ as a light green band in Fig. 2 to demonstrate the impact of changing the prior strength, and because it is a model that has the same Bayesian evidence as ΛCDM while deviating from Λ at a 2.7σ confidence level. Conversely, our forecast for DESI++ shows that, if the $w(z)$CDM model was true, it would be decisively supported by Bayesian evidence over a wide range of prior strengths, as shown in Fig. 3.

Various ways to relieve the tension between datasets have been proposed, including allowing for additional relativistic degrees of freedom[27], massive neutrinos[27] and an interacting vacuum[28,29]. In addition, to relieve the tension between the ΛCDM parameters required to fit the CMB temperature anisotropy spectrum at large and small scales, the Planck team introduced[7] a parameter, $A_{\rm Lens}$, which rescales the amplitude of the weak-lensing contribution to the temperature power spectrum. In the $w(z)$ reconstruction discussed earlier, we fixed $A_{\rm Lens}=1$, assumed that neutrinos are massless and set the effective number of relativistic species at the standard ΛCDM value of $N_{\rm eff}=3.04$. We have checked the effect of these parameters on the reconstructed $w(z)$ by considering model M_1, with neutrino mass, M_ν, fixed to 0.06 eV; model M_2, with M_ν and $N_{\rm eff}$ added as free parameters; and model M_3, with varied $A_{\rm Lens}$. In all these cases, we find that the shape of the reconstructed $w(z)$ and the significance of its deviation from -1 are practically the same. The inferred values of the cosmological parameters in these models are given in Supplementary Table 3, and the corresponding reconstructed $w(z)$ values are shown in Supplementary Fig. 5. The Bayes factors for M_1, M_2 and M_3 relative to the corresponding ΛCDM models (with the same added parameters) are shown in Table 3. We also checked that neither the constant w model (M_4) nor the linear (w_0, w_a) parametrization of w (M_5) is capable of releasing the tensions between all datasets simultaneously (see Table 1). Interestingly, we find that our dark energy model with a non-parametrically reconstructed $w(z)$ has a larger Bayes factor than that of w_0w_aCDM despite the latter having only two parameters (see results for M_4 and M_5 in Table 3).

There is always a possibility that the tensions between datasets, quantified in terms of the KL divergence in this work, are due to as-yet-unknown systematic effects. However, it is intriguing that they persist with improvements in the quantity and the quality of the data[10,11,30]. If interpreted as a manifestation of dark energy dynamics, they suggest a $w(z)$ that crosses -1 and has a shape that is representative of modified-gravity models. The commonly used (w_0, w_a) parametrization would have missed this behaviour and has a lower Bayesian evidence than the reconstructed $w(z)$ model, despite the latter having more degrees of freedom. Thus, our results demonstrate that the current data can provide non-trivial constraints on the dark energy dynamics. It is also intriguing that the evidence for $w(z)\neq-1$, while below that of ΛCDM, has become stronger with the new independent data added since 2012, and that the ALL16 reconstruction is consistent with the ALL12 $w(z)$. We emphasize that we have not optimized the prior to maximize either the Bayes ratio or the statistical significance of the departure from -1, as it would be contrary to the principles of Bayesian inference. Future data have the ability to confirm conclusively the dark energy evolution inferred in this work if it happened to be the true model.

Methods

Tension calculation. The KL divergence[13], also known as relative entropy, has been extensively used as a way of quantifying the degree of tension between different datasets within the ΛCDM model[15,31–37]. Rather than focusing on particular model parameters, it is designed to compare the overall concordance of datasets within a given model. Alternative methods of quantification of the tension have been discussed in the literature[8,38].

The KL divergence quantifies the proximity of two PDFs, P_1 and P_2, of a multi-dimensional random variable θ. If both P_1 and P_2 are assumed to be Gaussian[15], and data are assumed to be more informative than the priors, we can write the difference between the actual and the expected KL divergence, called the 'Surprise'[15], as

$$S=\frac{1}{2\ln2}[(\theta_1-\theta_2)^T\mathcal{C}_1^{-1}(\theta_1-\theta_2)-\mathrm{tr}(\mathcal{C}_2\mathcal{C}_1^{-1}+\mathrm{I})] \quad (1)$$

where θ_1 and θ_2 are the best-fit parameter vectors, C_1 and C_2 are the covariance matrices for P_1 and P_2, and I is the unity matrix. The standard deviation of the expected KL divergence is

$$\Sigma=\frac{1}{\sqrt{2\ln2}}\sqrt{\mathrm{tr}(\mathcal{C}_2\mathcal{C}_1^{-1}+\mathrm{I})^2} \quad (2)$$

We can quantify the tension, T, between P_1 and P_2 in terms of the signal-to-noise ratio, as $T=S/\Sigma$. If $T\lesssim1$, then P_1 and P_2 are consistent with each other[32].

Datasets used. The datasets we consider include the Planck 2015 (P15) CMB temperature and polarization auto- and cross-angular power spectra[7], the Joint Light-curve Analysis SNe[39] (JLA), the 6dFRS (6dF)[40] and SDSS main galaxy sample[41] BAO measurements, the WiggleZ galaxy power spectra[42] in four redshift slices containing information about the BAO and redshift-space distortions ($P(k)$), the weak-lensing shear angular power spectra in six redshift slices from CFHTLenS[43] (WL), the recent estimate of H_0 obtained from local measurements of Cepheids[12] (H_0), the $H(z)$ measurements using the relative age of old and passively evolving galaxies following a cosmic chronometer approach[44] (OHD), the BOSS DR12 'Consensus' BAO and redshift-space distortion measurements using the complete BOSS DR12 sample covering the redshift range of $0.2<z<0.75$ at three effective redshifts (BAO-3z)[45], the BAO measurements using the same galaxy sample but at nine effective redshifts[23] (BAO-9z), and the LyαFB measurements[3]. A summary of datasets and data combinations used in this work is shown in Supplementary Table 1.

We account for the systematic effects in our analysis as implemented in the public likelihood codes. However, we note that there may be additional systematic effects. For example, the relative velocity between baryons and dark matter may affect the BAO distance measurements[46]. This effect is estimated to be at subpercent level for the galaxy BAO measurements of BOSS[47,48] and is currently unknown for LyαFB. For SNe, we use the conventional χ^2 statistics for the analysis, although alternative statistics may extract more information and reduce the systematic effects for the JLA sample to some extent[49,50].

Non-parametric $w(z)$ reconstruction. To start, $w(z)$ is parameterized in terms of its values at discrete steps in z, or the scale factor a. Fitting a large number of uncorrelated bins would result in extremely large uncertainties and, in fact, would prevent the Markov chain Monte Carlo samples from converging because of the many degenerate directions in parameter space. Conversely, fitting only a few bins could significantly bias the result. Our approach is to introduce a prior covariance between the bins based on a specified two-point function that correlates values of w at different a, $\xi_w(|a-a'|)\equiv\langle(w[a]-w^{\rm fid}[a])(w[a']-w^{\rm fid}[a'])\rangle$ (where $w^{\rm fid}$ is the

fiducial model), which can be taken to be of the form proposed in ref. [51], $\xi_{\rm CPZ}(\delta a)=\xi_w(0)/(1+[\delta a/a_c]^2)$, where a is the scale factor of the Universe and $\xi_w(0)$ is a normalization factor set by the expected variance in the mean w, σ_w^2. As shown in ref. [17], results are largely independent of the choice of the correlation function. The prior covariance matrix C is obtained by projecting $\xi_w(|a-a'|)$ onto the discrete w-bins[17,51], and the prior PDF is taken to be of Gaussian form: $\mathcal{P}_{\rm prior}(w)\propto\exp[-(w-w^{\rm fid})^T C^{-1}(w-w^{\rm fid})/2]$. The reconstructed model is that which maximizes the posterior probability, which by Bayes' theorem is proportional to the likelihood of the data multiplied by the prior probability, $\mathcal{P}(w|D)\propto\mathcal{P}(D|w)\times\mathcal{P}_{\rm prior}(w)$. Effectively, the prior results in a new contribution to the total χ^2 of a model, which penalizes models that are less smooth.

In our reconstruction of $w(z)$, we set $a_c=0.06$ and $\sigma_w=0.04$, which is the 'weak prior' used by Zhao et al.[21]. To calculate the observables, we use a version of Code for Anisotropies in the Microwave Background[52] modified to include dark energy perturbations for an arbitrary w[53]. We use PolyChord[54], which is a nested sampling plug-in for CosmoMC[55], to sample the parameter space $P\equiv(\omega_b,\omega_c,\Theta_s,\tau,n_s,A_s,w_1,\ldots,w_{30},\mathcal{N})$ where ω_b and ω_c are the baryon and CDM densities, Θ_s is the angular size of the sound horizon at decoupling, τ is the optical depth, n_s and A_s are the spectral index and the amplitude of the primordial power spectrum, respectively, and $w_1,\ldots,w_{30}$ denote the 30 w-bin parameters. The first 29 w-bins are uniform in $a\in(0.286,1)$, corresponding to $z\in(0,2.5)$, and the last wide bin covers $z\in(2.5,1100)$. We marginalize over nuisance parameters such as the intrinsic supernova luminosity.

Principal-component analysis of $w(z)$. First, we diagonalize the posterior covariance of w-bins to find their uncorrelated linear combinations (eigenmodes), along with the eigenvalues, which quantify how well a given eigenmode is constrained[56]. We plot the inverse eigenvalues of the posterior covariance, ordered according to the number of nodes in the eigenmodes, in Supplementary Fig. 3a. The number of nodes is representative of the smoothness in the evolution of eigenmodes, with the first four posterior eigenmodes shown in Supplementary Fig. 3b. Next, we perform a principal-component analysis of the prior covariance matrix and plot its inverse eigenvalues alongside those of the posterior. We see that the fifth and higher number eigenvalues of the two matrices coincide, which means that they are fully determined by the prior. However, the first four inverse eigenvalues of the posterior are significantly larger than that of the prior, indicating that they are constrained primarily by the data. This is precisely the intent of the correlated prior method: the smooth features in $w(z)$ are constrained by the data, with no bias induced by the prior, while the high-frequency features are constrained by the prior. Thus, our $w(z)$CDM model effectively has only four additional degrees of freedom compared with ΛCDM.

Dependence of the result on the correlated prior. To investigate the dependence of our result on the strength of the correlated prior, in Fig. 3, we plot the Bayes factor and the statistical significance of $w\neq-1$ as a function of $\sigma_{\rm D}$, which is a parameter that is added to the inverse covariance matrix of the correlated prior effectively to strengthen it. We find that neither the ALL12 nor the ALL16 dataset provides evidence for a dynamical dark energy at all prior strengths, although the Bayes factor for ALL16 is generally much less negative than that of ALL12 for all priors. For example, the Bayes factor grows from -6.7 ± 0.3 to -3.3 ± 0.3 using ALL12 and ALL16 respectively, which corresponds to $\sigma_{\rm D}=3$. Conversely, the plot shows that, if the $w(z)$CDM model was true, DESI++ would be able to provide a decisive Bayesian evidence over a wide range of prior strengths.

Data availability. The data that support the plots within this paper and other findings of this study are available from the corresponding author upon reasonable request.

Received: 3 March 2017; Accepted: 3 July 2017;
Published online: 28 August 2017

References

1. Riess, A. G. et al. Observational evidence from supernovae for an accelerating universe and a cosmological constant. *Astron. J.* **116**, 1009–1038 (1998).
2. Perlmutter, S. et al. Measurements of Ω and Λ from 42 high-redshift supernovae. *Astrophys. J.* **517**, 565–586 (1999).
3. Delubac, T. et al. Baryon acoustic oscillations in the Lyα forest of BOSS DR11 quasars. *Astron. Astrophys.* **574**, A59 (2015).
4. Sahni, V., Shafieloo, A. & Starobinsky, A. A. Model-independent evidence for dark energy evolution from baryon acoustic oscillations. *Astrophys. J. Lett.* **793**, L40 (2014).
5. Battye, R. A., Charnock, T. & Moss, A. Tension between the power spectrum of density perturbations measured on large and small scales. *Phys. Rev. D* **91**, 103508 (2015).
6. Aubourg, É. et al. Cosmological implications of baryon acoustic oscillation measurements. *Phys. Rev. D* **92**, 123516 (2015).
7. Planck Collaboration et al. Planck 2015 results. XIII. Cosmological parameters. *Astron. Astrophys.* **594**, A13 (2016).
8. Raveri, M. Are cosmological data sets consistent with each other within the Λ cold dark matter model? *Phys. Rev. D* **93**, 043522 (2016).
9. Addison, G. E. et al. Quantifying discordance in the 2015 Planck CMB spectrum. *Astrophys. J.* **818**, 132 (2016).
10. Bernal, J. L., Verde, L. & Riess, A. G. The trouble with H_0. *J. Cosmol. Astropart. Phys.* **10**, 019 (2016).
11. Freedman, W. L. Cosmology at a crossroads. *Nat. Astron.* **1**, 0121 (2017).
12. Riess, A. G. et al. A 2.4% determination of the local value of the Hubble constant. *Astrophys. J.* **826**, 56 (2016).
13. Kullback, S. & Leibler, R. A. On information and sufficiency. *Ann. Math. Stat.* **22**, 79 (1951).
14. DESI Collaboration et al. The DESI experiment part I: science, targeting, and survey design. Preprint at https://arxiv.org/abs/1611.00036 (2016).
15. Seehars, S., Amara, A., Refregier, A., Paranjape, A. & Akeret, J. Information gains from cosmic microwave background experiments. *Phys. Rev. D* **90**, 023533 (2014).
16. Linder, E. V. Exploring the expansion history of the Universe. *Phys. Rev. Lett.* **90**, 091301 (2003).
17. Crittenden, R. G., Zhao, G.-B., Pogosian, L., Samushia, L. & Zhang, X. Fables of reconstruction: controlling bias in the dark energy equation of state. *J. Cosmol. Astropart. Phys.* **2**, 048 (2012).
18. Vikman, A. Can dark energy evolve to the phantom? *Phys. Rev. D* **71**, 023515 (2005).
19. Feng, B., Wang, X. & Zhang, X. Dark energy constraints from the cosmic age and supernova. *Phys. Lett. B* **607**, 35–41 (2005).
20. Das, S., Corasaniti, P. S. & Khoury, J. Superacceleration as the signature of a dark sector interaction. *Phys. Rev. D* **73**, 083509 (2006).
21. Zhao, G.-B., Crittenden, R. G., Pogosian, L. & Zhang, X. Examining the evidence for dynamical dark energy. *Phys. Rev. Lett.* **109**, 171301 (2012).
22. Reid, B. A. et al. The clustering of galaxies in the SDSS-III Baryon Oscillation Spectroscopic Survey: measurements of the growth of structure and expansion rate at z=0.57 from anisotropic clustering. *Mon. Not. R. Astron. Soc.* **426**, 2719–2737 (2012).
23. Zhao, G.-B. et al. The clustering of galaxies in the completed SDSS-III Baryon Oscillation Spectroscopic Survey: tomographic BAO analysis of DR12 combined sample in Fourier space. *Mon. Not. R. Astron. Soc.* **466**, 762–779 (2017).
24. Riess, A. G. et al. A redetermination of the Hubble constant with the Hubble Space Telescope from a differential distance ladder. *Astrophys. J.* **699**, 539–563 (2009).
25. Larson, D. et al. Seven-year Wilkinson Microwave Anisotropy Probe (WMAP) observations: power spectra and WMAP-derived parameters. *Astrophys. J. Suppl.* **192**, 16 (2011).
26. Astier, P., Guy, J., Pain, R. & Balland, C. Dark energy constraints from a space-based supernova survey. *Astron. Astrophys.* **525**, A7 (2011).
27. Di Valentino, E., Melchiorri, A. & Silk, J. Reconciling Planck with the local value of H_0 in extended parameter space. *Phys. Lett. B* **761**, 242–246 (2016).
28. Solà, J., Gómez-Valent, A. & de Cruz Pérez, J. First evidence of running cosmic vacuum: challenging the concordance model. *Astrophys. J.* **836**, 43 (2017).
29. Wang, Y., Zhao, G.-B., Wands, D., Pogosian, L. & Crittenden, R. G. Reconstruction of the dark matter–vacuum energy interaction. *Phys. Rev. D* **92**, 103005 (2015).
30. Bautista, J. E. et al. Measurement of BAO correlations at z=2.3 with SDSS DR12 Lyα-forests. Preprint at https://arxiv.org/abs/1702.00176 (2017).
31. Grandis, S., Seehars, S., Refregier, A., Amara, A. & Nicola, A. Information gains from cosmological probes. *J. Cosmol. Astropart. Phys.* **5**, 034 (2016).
32. Seehars, S., Grandis, S., Amara, A. & Refregier, A. Quantifying concordance in cosmology. *Phys. Rev. D* **93**, 103507 (2016).
33. Raveri, M., Martinelli, M., Zhao, G. & Wang, Y. Information gain in cosmology: from the discovery of expansion to future surveys. Preprint at https://arxiv.org/abs/1606.06273 (2016).
34. Paykari, P. & Jaffe, A. H. Sparsely sampling the sky: a Bayesian experimental design approach. *Mon. Not. R. Astron. Soc.* **433**, 3523–3533 (2013).
35. Kunz, M., Trotta, R. & Parkinson, D. R. Measuring the effective complexity of cosmological models. *Phys. Rev. D* **74**, 023503 (2006).
36. Amara, A. & Refregier, A. Model breaking measure for cosmological surveys. *Phys. Rev. D* **89**, 083501 (2014).
37. Verde, L., Protopapas, P. & Jimenez, R. The expansion rate of the intermediate universe in light of Planck. *Phys. Dark Univ.* **5**, 307–314 (2014).
38. Charnock, T., Battye, R. A. & Moss, A. Planck confronts large scale structure: methods to quantify discordance. Preprint at https://arxiv.org/abs/1703.05959 (2017).
39. Betoule, M. et al. Improved cosmological constraints from a joint analysis of the SDSS-II and SNLS supernova samples. *Astron. Astrophys.* **568**, A22 (2014).
40. Beutler, F. et al. The 6dF Galaxy Survey: baryon acoustic oscillations and the local Hubble constant. *Mon. Not. R. Astron. Soc.* **416**, 3017–3032 (2011).

41. Ross, A. J. et al. The clustering of the SDSS DR7 main galaxy sample - I. A 4 per cent distance measure at z=0.15. *Mon. Not. R. Astron. Soc.* **449**, 835–847 (2015).
42. Parkinson, D. et al. The WiggleZ Dark Energy Survey: final data release and cosmological results. *Phys. Rev. D* **86**, 103518 (2012).
43. Heymans, C. et al. CFHTLenS tomographic weak lensing cosmological parameter constraints: mitigating the impact of intrinsic galaxy alignments. *Mon. Not. R. Astron. Soc* **432**, 2433–2453 (2013).
44. Moresco, M. et al. A 6% measurement of the Hubble parameter at z∼0.45: direct evidence of the epoch of cosmic re-acceleration. *J. Cosmol. Astropart. Phys.* **5**, 014 (2016).
45. Alam, S. et al. The clustering of galaxies in the completed SDSS-III Baryon Oscillation Spectroscopic Survey: cosmological analysis of the DR12 galaxy sample. Preprint at https://arxiv.org/abs/1607.03155 (2016).
46. Dalal, N., Pen, U.-L. & Seljak, U. Large-scale BAO signatures of the smallest galaxies. *J. Cosmol. Astropart. Phys.* **11**, 007 (2010).
47. Beutler, F., Seljak, U. & Vlah, Z. Constraining the relative velocity effect using the Baryon Oscillation Spectroscopic Survey. Preprint at https://arxiv.org/abs/1612.04720 (2016).
48. Slepian, Z. et al. Constraining the baryon–dark matter relative velocity with the large-scale 3-point correlation function of the SDSS BOSS DR12 CMASS galaxies. Preprint at https://arxiv.org/abs/1607.06098 (2016).
49. Ma, C., Corasaniti, P.-S. & Bassett, B. A. Application of Bayesian graphs to SN Ia data analysis and compression. *Mon. Not. R. Astron. Soc.* **463**, 1651–1665 (2016).
50. Shafieloo, A., Clifton, T. & Ferreira, P. The crossing statistic: dealing with unknown errors in the dispersion of type Ia supernovae. *J. Cosmol. Astropart. Phys.* **8**, 017 (2011).
51. Crittenden, R. G., Pogosian, L. & Zhao, G.-B. Investigating dark energy experiments with principal components. *J. Cosmol. Astropart. Phys.* **12**, 025 (2009).
52. Lewis, A., Challinor, A. & Lasenby, A. Efficient computation of cosmic microwave background anisotropies in closed Friedmann–Robertson–Walker models. *Astrophys. J.* **538**, 473–476 (2000).
53. Zhao, G.-B., Xia, J.-Q., Li, M., Feng, B. & Zhang, X. Perturbations of the Quintom models of dark energy and the effects on observations. *Phys. Rev. D* **72**, 123515 (2005).
54. Handley, W. J., Hobson, M. P. & Lasenby, A. N. POLYCHORD: nested sampling for cosmology. *Mon. Not. R. Astron. Soc.* **450**, L61–L65 (2015).
55. Lewis, A. & Bridle, S. Cosmological parameters from CMB and other data: a Monte Carlo approach. *Phys. Rev. D* **66**, 103511 (2002).
56. Huterer, D. & Starkman, G. Parametrization of dark energy properties: a principal component approach. *Phys. Rev. Lett.* **90**, 031301 (2003).

Acknowledgements

G.-B.Z. is supported by National Natural Science Foundation of China (NSFC) Grant No. 11673025, and by a Royal Society-Newton Advanced Fellowship. G.-B.Z. and Y.W. are supported by National Astronomical Observatories, Chinese Academy of Sciences, and by University of Portsmouth. M.R. is supported by US Department of Energy contract DE-FG02-13ER41958. M.R. acknowledges partial support, during the development of this work, by the Italian Space Agency (ASI) through the ASI contracts Euclid-IC (I/031/10/0) and the INFN-INDARK initiative. M.R. thanks Scuola Internazionale Superiore di Studi Avanzati, where part of this work was completed. L.P. is supported by The Natural Sciences and Engineering Research Council of Canada, R.C. by Science and Technology Facilities Council grant ST/H002774/1, and Y.W. by NSFC Grant No. 11403034. G.R. acknowledges support from the National Research Foundation of Korea (NRF) through NRF-SGER 2014055950 funded by the Korean Ministry of Education, Science and Technology (MoEST), and from the faculty research fund of Sejong University in 2016. A.S. would like to acknowledge the support of the National Research Foundation of Korea (NRF - 2016R1C1B2016478). Funding for SDSS-III has been provided by the Alfred P. Sloan Foundation, the Participating Institutions, the National Science Foundation and the US Department of Energy Office of Science. The SDSS-III website is http://www.sdss3.org/. SDSS-III is managed by the Astrophysical Research Consortium for the Participating Institutions of the SDSS-III Collaboration including the University of Arizona, the Brazilian Participation Group, Brookhaven National Laboratory, Carnegie Mellon University, University of Florida, the French Participation Group, the German Participation Group, Harvard University, the Instituto de Astrosica de Canarias, the Michigan State/Notre Dame/JINA Participation Group, Johns Hopkins University, Lawrence Berkeley National Laboratory, Max Planck Institute for Astrophysics, Max Planck Institute for Extraterrestrial Physics, New Mexico State University, New York University, Ohio State University, Pennsylvania State University, University of Portsmouth, Princeton University, the Spanish Participation Group, University of Tokyo, University of Utah, Vanderbilt University, University of Virginia, University of Washington and Yale University.

Author contributions

G.-B.Z. proposed the idea, performed the dark energy reconstruction, evidence calculation, principal-component analysis and tension calculation. M.R. and Y.W. contributed to the tension calculation. G.-B.Z. and L.P. wrote the draft, and all other co-authors commented on and helped to improve the manuscript and/or contributed to the BOSS data analysis.

Competing interests

The authors declare no competing financial interests.

Additional information

Supplementary information is available for this paper at doi:10.1038/s41550-017-0216-z.

Reprints and permissions information is available at www.nature.com/reprints.

Correspondence and requests for materials should be addressed to G.-B.Z.

Publisher's note: Springer Nature remains neutral with regard to jurisdictional claims in published maps and institutional affiliations.